Electronic Supplementary Information

Distinct seed topologies enable comparison of elongation and secondary nucleation pathways in seeded supramolecular polymerization

Hiroki Itabashi,[a] Keigo Tashiro,[b] Shumpei Koshikawa,[a] Sougata Datta,[c] and Shiki Yagai *[c,d]

[a] Division of Advanced Science and Engineering, Graduate School of Engineering, Chiba University, 1-33 Yayoi-cho, Inage-ku, Chiba 263-8522, Japan.
[b] Department of Applied Chemistry, Faculty of Science and Technology, Seikei University, 3-3-1, Kichijoji-kitamachi, Musashino-shi, Tokyo, 180-8633, Japan.
[c] Institute for Advanced Academic Research (IAAR), Chiba University, 1-33, Yayoi-cho, Inage-ku, Chiba 263-8522, Japan.
[d] Department of Applied Chemistry and Biotechnology, Graduate School of Engineering, Chiba University, 1-33 Yayoi-cho, Inage-ku, Chiba 263-8522, Japan.

E-mail: yagai@faculty.chiba-u.jp

This PDF file includes:

Supplementary methods

Materials

Compound **2** was synthesized by following procedures shown in scheme S1. All commercially available reagents and solvents were of reagent grade and used without further purification. Spectroscopic grade solvents were used for spectroscopic measurements without further purification.

Nuclear magnetic resonance (NMR) spectroscopy, electrospray ionization mass (ESI-MS)

^{1}H and ^{13}C spectra were recorded on Bruker DPX 300 spectrometer and JEOL JMN-ECA500 NMR spectrometer.^{1}H NMR chemical shifts are reported in parts per million (ppm, δ) with the signal of tetramethylsilane (TMS) as internal standard at 0.00 ppm. The resonance multiplicity was represented in terms of s (singlet), d (doublet), m (multiplet), and brs (broad singlet). ^{13}C NMR chemical shifts reported in ppm (δ) were normalized with the chemical shifts of $CDCl_3$ at 77.16 ppm, DMSO-d_6 at 39.52 ppm, and THF-d_8 at 67.21 and 25.31 ppm as reference, respectively. ESI-MS and APCI-MS spectra measurements were conducted on Thermo Scientific Exactive.

UV-vis spectroscopy

UV-vis absorption spectra were measured by JASCO V660 and V760 spectrophotometers equipped with JASCO ETCS-761 temperature-control unit using screw-capped quartz cuvettes with 1.0-cm optical path-length.

Atomic force microscopy (AFM)

AFM imaging was carried out under ambient conditions using Multimode 8 Nanoscope V (Bruker) in Peak Force Tapping (ScanAsyst) mode. Silicon cantilevers (SCANASYST-AIR) with a spring constant of 0.4 N/m and frequency of 70 kHz (nominal value, Bruker, Japan) were used. The samples were prepared by spin-coating (3000 rpm, 1 min) of solution (10 μL) of supramolecular polymers onto freshly cleaved highly oriented pyrolytic graphite (HOPG, 5 mm × 5 mm) at 293 K. Images were processed using NanoScope Analysis 3.00 (Bruker Instruments) and ImageJ v1.53s (National Institutes of Health).

Dynamic light scattering (DLS)

DLS measurements were performed on Zetasizer Nano S (Malvern Instruments) device using non-invasive back-scatter technology (NIBS) with He-Ne laser (633 nm, 4.0 mW). The scattering angle was set at 173°.

Quantum Chemical Calculation

Quantum chemical calculation was performed by using Gaussian 16W program package[S1] and visualization of molecular electrostatic potential was carried out by GaussView 6.0 program. Structural optimizations for both **1** and **2** in MCH were executed by following density functional theory (DFT) with B3LYP/6-31G(d) basis set accompanying integral equation formalism polarizable continuum model (IEF-PCM) to consider solvent effect.

Preparation of $\mathbf{SP_{helicoid}}$ seed

A $\mathbf{SP}_{\mathrm{helicoid}}$ solution was initially prepared by cooling a hot MCH solution of **2** ($c = 1.0 \times 10^{-5}$ M) from 373 K 293 K at a cooling rate of 1.0 K min^{-1}. The $\mathbf{SP}_{\mathrm{helicoid}}$ solution was sonicated for 15 s at 293 K to give a short $\mathbf{SP}_{\mathrm{helicoid}}$ solution. After evaporation of MCH under reduced pressure, the residue was dissolved in toluene/MCH = 40:60 (v/v) mixture to give a $\mathbf{SP}_{\mathrm{helicoid}}$ seed solution (Fig. S7).

Preparation of $\mathbf{SP_{ring}}$ seed

A monomeric solution of **2** in $CHCl_3$ ($c = 1.0 \times 10^{-3}$ M, 100 μL) was injected into 900 μL of pure MCH at 293 K. The resulting MCH:$CHCl_3$ = 90:10 v/v solution (1 mL, $c = 1.0 \times 10^{-4}$ M) was heated to 363 K and then cooled to 303 K to re-organize relatively shorter open-ended species into highly elongated $\mathbf{SP}_{\mathrm{helicoid}}$. The resulting solution was passed through a membrane filter of 200 nm pore size (Millex-LG, Merck Millipore) to filter out the elongated $\mathbf{SP}$s$_{\mathrm{helicoid}}$ from $\mathbf{SP}_{\mathrm{ring}}$. The filtrate was evaporated and the residue was re-dissolved in toluene/MCH =40:60 (v/v) mixture to give the $\mathbf{SP}_{\mathrm{ring}}$ seed solution (Fig. S9).

Estimation of degree of aggregation (α_{agg})

Using the temperature-dependent UV/vis absorption data, the degree of aggregation (α_{agg}) at a given temperature (T) was calculated from Supplementary Equation S1:

$$\alpha_{\mathrm{agg}}(T) = \frac{\varepsilon(T) - \varepsilon_{\mathrm{mon}}}{\varepsilon_{\mathrm{agg}} - \varepsilon_{\mathrm{mon}}} \qquad \text{(S1)}$$

where $\varepsilon_{\mathrm{agg}}$ and $\varepsilon_{\mathrm{mon}}$ are molar absorption coefficients at 470 nm of fully aggregated (the highest value, $\alpha_{\mathrm{agg}} = 1$) and pure monomeric species (the lowest value, $\alpha_{\mathrm{agg}} = 0$), respectively, and $\varepsilon(T)$ is the molar absorption coefficient at a given temperature.

Cooperative (nucleation-elongation) model fitting

Cooperative assembly processes were analyzed by nucleation-elongation model proposed by Meijer and co-workers.[S2] when the plot of degree of aggregation (α_{agg}) versus T is non-sigmoidal, the polymerization process can be followed by cooperative model.
In the elongation regimes ($T < T_{\mathrm{e}}$) were fitted with Supplementary Equation S2:

$$a_{\mathrm{agg}} = a_{\mathrm{SAT}} \left[1 - \exp\left(-\frac{\Delta H_e}{\mathrm{R}{T_e}^2}\,(T - T_e)\right)\right] \tag{S2}$$

where ΔH_{e} is the enthalpy release in the elongation regime, α_{SAT} is a parameter the correction coefficient, R is the ideal gas constant, and T_e is critical temperature.

Growth curve fitting

The time-dependent growth kinetics of the supramolecular polymers were fitted using AmyloFit software (http://www.amylofit.ch.cam.ac.uk) developed by Knowles group.[S3] The mathematical models used for fitting the experimental data were analytical solutions derived by Knowles and co-workers. The mathematical models used in this study are as follows:

Seed induced nucleation elongation model:

The growth curve upon addition of **SP**$_{\mathrm{helicoid}}$ seeds was fitted with the seed induced nucleation elongation model defined by Supplementary Equation S3:

$$\frac{M}{m_t} = 1 - \frac{m_0}{m_t}\left[\frac{1}{\mu}\cosh\left(\sqrt{\frac{n_c}{2}}\mu\lambda t + \nu\right)\right]^{-\frac{2}{n_c}} \tag{S3}$$

In this equation, parameters λ, β, μ, and ν are further defined as follows:

$$\lambda = \sqrt{2k_+k_n{m_0}^{n_c}} \tag{S4}$$

$$\beta = \sqrt{\frac{k_+ n_c}{k_n {m_0}^{n_c}} P_0} \tag{S5}$$

$$\mu = \sqrt{1 + \beta^2} \tag{S6}$$

$$\nu = \log(\beta + \mu) \tag{S7}$$

In the above equations, M is the polymerized monomer mass concentration, m_t is the total monomer concentration, m_0 is the initial monomer concentration, n_c is the reaction order of primary nucleation, t is the time, k_+ is the elongation rate constant, k_n is the primary nucleation rate constant, P_0 is the initial number concentration of aggregates.

Secondary nucleation elongation model:

The growth curves of unseeded and **SP**ring-seeded systems were fitted with the secondary nucleation elongation model defined as Supplementary Equation S8:

$$\frac{M}{M_\infty} = 1 - \left(1 - \frac{M_0}{M_\infty}\right) e^{-k_\infty t} \cdot \left(\frac{B_- + C_+ e^{\kappa t}}{B_+ + C_+ e^{\kappa t}} \cdot \frac{B_+ + C_+}{B_- + C_+}\right)^{\frac{k_\infty}{\kappa k_\infty}} \tag{S8}$$

where parameters κ, $C_\pm$, k_∞, $\bar{k}_\infty$, and $B_\pm$ are further defined as follows:

$$\kappa = \sqrt{2 m_0 k_+ {m_0}^{n_2} k_2} \tag{S9}$$

$$C_\pm = \frac{k_+ P_0}{\kappa} \pm \frac{k_+ M_0}{2 m_0 k_+} \pm \frac{\lambda^2}{2\kappa^2} \tag{S10}$$

$$k_\infty = \sqrt{(2k_+ P(0))^2 + \frac{4 k_+ k_n {m_0}^{n_c}}{n_c} + \frac{4 k_+ k_2 m_\mathrm{t} {m_0}^{n_2}}{n_2} + \frac{4 k_+ k_2 {m_0}^{n_2+1}}{n_2 + 1}} \tag{S11}$$

$$\bar{k}_\infty = \sqrt{{k_\infty}^2 - 2 C_+ C_- \kappa^2} \tag{S12}$$

$$B_\pm = \frac{k_\infty \pm \bar{k}_\infty}{2\kappa} \tag{S13}$$

In the above equiations, M_∞ is the polymerized monomer mass concentration at long time, n_2 is the reaction order of secondary nucleation, k_2 is the secondary nucleation rate constant.

We selected the mathematical models which could fit most accurately to each growth curve. Because the same experimental conditions were applied except for the added seeds, n_c was defined as a global parameter. For the **SP**$_{\text{helicoid}}$-seeded experiment, we set 1.0×10^{-9} M as P_0 value by assuming that one seed is composed of ca. 10^4 of molecules based on the average columnar length of **SP**$_{\text{helicoid}}$ seeds (100–200 nm).

AFM image analysis of the monomer distribution ratio between SP$_{\text{random}}$ and SP$_{\text{ring}}$

The monomer distribution ratio between **SP**$_{\text{random}}$ and **SP**$_{\text{ring}}$ in the **SP**$_{\text{ring}}$-seeding experiment is estimated from AFM images by using ImageJ and following equation:

$$\text{The monomer distribution ratio (\%) of } \mathbf{SP}_{\text{random}}\ (\mathbf{SP}_{\text{ring}}) = \frac{\text{Total fiber length of } \mathbf{SP}_{\text{random}}\ (\mathbf{SP}_{\text{ring}})}{\text{Total fiber length of } \mathbf{SP}_{\text{random}} \text{ and } \mathbf{SP}_{\text{ring}}} \times 100$$

The total fiber length of **SP**$_{\text{random}}$ was estimated by tracing total **SP**$_{\text{random}}$ fibers in the AFM images (Fig. S12a). The total fiber length of **SP**$_{\text{ring}}$ was estimated from the number of **SP**$_{\text{ring}}$ with their average circumference (Fig. S12b).

Synthesis

Compound **2** was synthesized by following procedure as shown Scheme S1.

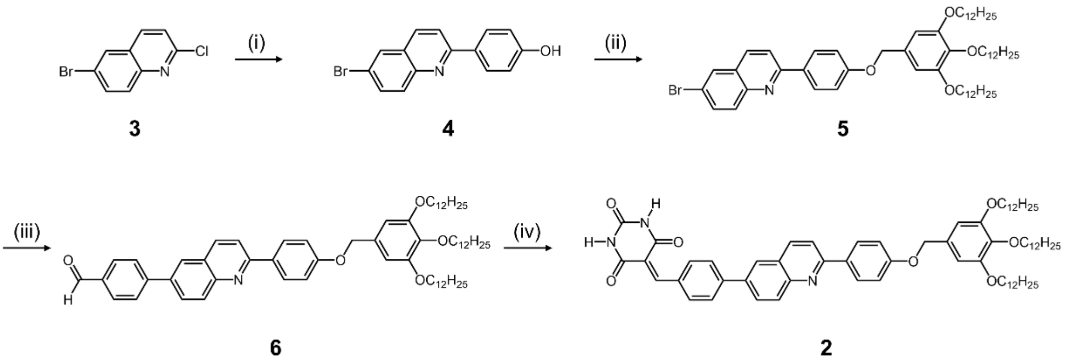

Scheme S1. Synthesis of compound **2**. i) 4-(4,4,5,5-tetramethyl-1,3,2-dioxaborolan-2yl)phenol, Pd(PPh_3)$_4$, Na_2CO_3, THF, water, 343 K, 12 h; ii) 5-(chloromethyl)-1,2,3-tris(dodecyloxy)benzene, K_2CO_3, DMF, 343 K, 12 h; iii) 4-formylphenyl boronic acid, $Pd_2(dba)_3$, $CHCl_3$, SPhos, Na_2CO_3, THF–water (4:1 v/v), 70 °C, 3 h; iv) barbituric acid, ethanol, reflux, 12 h.

4-(6-bromoquinolin-2-yl)phenol (4)

Compound **3** (450 mg, 1.86 mmol), tetrakis(triphenylphosphine)palladium(0) (Pd(PPh_3)$_4$, 107 mg, 0.09 mmol, 5 mol% to **3**) and 4-hydroxyphenilboronic acid (260 mg, 1.86 mmol) was added to a 100-mL three-neck round bottom flask connected with a refluxing condenser. The flask was evacuated and refilled with N_2 gas three times. 2 M of Na_2CO_3 *aq*. (10 mL) and dry tetrahydrofuran (THF, 30 mL) were added to the flask and then the mixture was stirred at 343 K for 12 h. The mixture was then passed through a small pad celite column. The obtained crude product was purified by silica gel column chromatography using a mixed solvent of ethyl acetone–hexane (5:95 v/v) as the eluent. Appropriate fractions were collected and evaporation of the solvent to give compound **4** as a yellow solid (390 mg, 70 % of yield). ^{1}H NMR (300 MHz, DMSO-d_6, 293 K): δ9.92 (s, 1H), 8.36 (d, 1H, J = 8.6 Hz), 8.24 (d, J = 2.2, 1H), 8.15 (d, J = 8.6, 2H), 8.11 (d, J = 8.8 Hz, 1H), 7.94 (d, 1H, 8.8 Hz), 7.84 (dd, J = 8.6, 2.2 Hz, 1H), 6.92 (d, J = 8.6, 2H) ppm. ^{13}C NMR (100 MHz, DMSO-d_6, 293 K): δ159.82, 157.10, 146.65, 136.54, 133.17, 131.42, 130.17, 129.61, 129.31, 128.30, 119.52, 118.93, 116.16 ppm. HRMS (ESI): m/z calcd for $C_{15}H_{11}ONBr$ 300.0019 [M+H]$^+$, found 300.0013.

6-bromo-2-(4-((3,4,5-tris(dodecyloxy)benzyl)oxy)phenyl)quinoline (5)

Compound **4** (250 mg, 0.367 mmol) was dissolved in a suspension of K_2CO_3 (250 mg, 0.404 mmol) in dry dimethylformamide (DMF, 10 mL) at 343 K. 3,4,5-Tri(*n*-dodecyloxy) benzyl chloride[S4] (103 mg, 0.404 mmol) dissolved in dry DMF (5 mL) was added dropwise to the suspension and the mixture was stirred at 343 K for 16 h. The reaction mixture was cooled with an ice-water bath and the resulting precipitates were collected by filtration. The crude product was purified by silica gel column chromatography using a mixed solvent of ethyl acetone–hexane (5:95 v/v) as the eluent. Appropriate fractions were collected and evaporated to give compound **5** as a yellow solid (277 mg, 80 % of yield). ^{1}H NMR (300 MHz, $CDCl_3$, 293 K): δ 8.13 (d, J = 8.8 Hz, 2H), 8.09 (d, J = 8.6 Hz, 1H), 7.99 (d, J = 8.9 Hz, 1H), 7.96 (d, J = 2.1 Hz, 1H), 7.85 (d, 8.7 Hz, 1H), 7.76 (dd, J = 8.9, 2.1 Hz, 1H), 7.11 (d, J = 8.8, 2H), 6.65 (s, 2H), 5.04 (s, 2H), 4.00–3.94 (m, 6H), 1.83–1.73 (m, 6H), 1.48–1.47 (m, 6H), 1.26 (m, 48H), 0.89–0.86 (m, 9H) ppm. ^{13}C NMR (100 MHz, $CDCl_3$, 293 K): δ 160.27, 157.06, 153.40, 146.89, 138.10, 135.55, 132.97, 131.95, 131.64, 131.27, 129.47, 128.87, 127.99, 119.60, 119.18, 115.22, 106.17, 73.47, 70.50, 69.18, 32.00, 31.99, 30.43, 29.83, 29.81, 29.77, 29.72, 29.49, 29.46, 29.43, 26.22, 26.18, 22.75, 14.17 ppm. HRMS (ESI): m/z calcd for $C_{58}H_{89}O_4NBr$ 942.5969 $[M+H]^+$, found 942.5951.

2-(4-((3,4,5-tris(dodecyloxy)benzyl)oxy)phenyl)quinoline-6-carbaldehyde (6)

Compound **5** (200 mg, 0.243 mmol), 4-formylphenylboronic acid (44 mg, 0.29 mmol), tris(dibenzylideneacetone)dipalladium(0)-chloroform adduct ($Pd_2(dba)_3{\cdot}CHCl_3$, 7.5 mg, 0.007 mmol, 3 mol% to **5**), dicyclohexyl(2',6'-dimethoxy-[1,1'-biphenyl]-2-yl)phosphane (SPhos, 5.98 mg, 0.015 mmol, 6 mol% to **5**), and Na_2CO_3 (77 mg, 0.729 mmol) were added to a 50 mL of three neck round bottom flask connected with a condenser. The flask was evacuated and refilled with N_2 gas three times. THF–water (4:1 mixture, 10 mL) was added to the flask, and the mixture was stirred at 343 K for 3 h. After the reaction mixture was diluted with chloroform, the resulting solution was washed with saturated NH_4Cl *aq*. and brine. The organic layer was dried over Na_2SO_4, and then the solvent was evaporated. The residue was purified by silica gel chromatography using $CHCl_3$ as an eluent. Appropriate fractions were collected and evaporated to give compound **6** as a yellow solid (212 mg, 90% of yield). ^{1}H NMR (300 MHz, $CDCl_3$, 293 K): δ 10.1 (s, 1H), 8.25 (d, J = 8.7 Hz, 1H), 8.23 (d, J = 8.9 Hz, 1H), 8.17 (d, J = 8.8 Hz, 2H), 8.06 (d, J = 2.0 Hz, 1H), 8.02 (d, J = 8.3 Hz, 2H), 8.00 (dd, J = 8.8, 2.0 Hz, 1H), 7.91 (dd, J = 8.6, 2.0 Hz, 3H), 7.13 (d, J = 8.8 Hz, 2H), 6.65 (s, 2H), 5.05 (s, 2H), 4.01–3.94 (m, 6H), 1.84–1.72 (m, 6H), 1.47 (m, 6H) 1.26 (m, 48H), 0.89–0.85 (m, 9H) ppm. ^{13}C NMR (100 MHz, $CDCl_3$, 293

K): δ 191.73, 160.27, 157.33, 153.40, 148.16, 146.33, 138.12, 136.96, 136.92, 135.40, 132.16, 131.65, 130.35, 128.94, 128.82, 127.83, 127.01, 125.97, 119.08, 115.25, 106.20, 73.47, 70.52, 69.20, 31.98, 31.96, 30.41, 29.80, 29.78, 29.75, 29.70, 29.48, 29.43, 29.40, 26.20, 26.16, 22.72, 14.14 ppm. HRMS (ESI): m/z calcd for $C_{65}H_{94}O_5N$ 968.7127 $[M+H]^+$, found 968.7105.

5-(4-(2-(4-((3,4,5-tris(dodecyloxy)benzyl)oxy)phenyl)quinolin-6-yl)benzylidene) pyrimidine-2,4,6(1H,3H,5H)-trione (2)

A mixture of **6** (100 mg, 0.103 mmol) and barbituric acid (66 mg, 0.516 mmol) in ethanol (20 mL) was refluxed at 343 K for 24 h. The reaction mixture was cooled to room temperature. The resulting precipitates were collected by filtration and repeatedly washed with hot ethanol to give pure compound **2** as a yellow solid (77.8 mg, 70 % of yield). ^{1}H NMR (500 MHz, $CDCl_3$, 333 K): δ 8.62 (s, 1H), 8.34 (d, *J* = 8.5 Hz, 2H), 8.21 (dd, *J* = 8.5, 2.4 Hz, 2H), 8.16 (d, *J* = 8.8 Hz, 2H), 8.07 (d, *J* = 2.0 Hz 1H), 8.00 (dd, *J* = 8.7, 2.1 Hz, 1H), 7.88 (d, *J* = 8.5 Hz, 1H), 7.87 (d, *J* = 8.5 Hz, 2H), 7.78 (brs, 1H), 7.67 (brs, 1H), 7.11 (d, *J* = 8.7 Hz, 2H), 6.64 (s, 2H), 5.04 (s, 2H), 4.00–3.94 (m, 6H), 1.80–1.73 (m, 6H), 1.47–1.45 (m, 6H) 1.26 (m, 48H), 0.88–0.86 (m, 9H) ppm. ^{13}C NMR (125 MHz, THF-d_8, 293 K): δ 163.15, 161.54, 160.53, 156.55, 154.67, 153.33, 149.63, 148.22, 144.13, 138.28, 136.83, 136.67, 134.93, 132.22, 132.03, 131.78, 130.08, 128.53, 128.30, 127.22, 126.47, 125.62, 118.30, 118.27, 114.69, 106.17, 72.59, 70.03, 68.77, 31.93, 31.91, 30.45, 29.82, 29.78, 29.70, 29.66, 29.55, 29.46, 29.36, 26.25, 26.17, 22.60, 13.47 ppm. HRMS (ESI): m/z calcd for $C_{69}H_{96}O_7N_3$ 1078.7243 $[M+H]^+$, found 1078.7228.

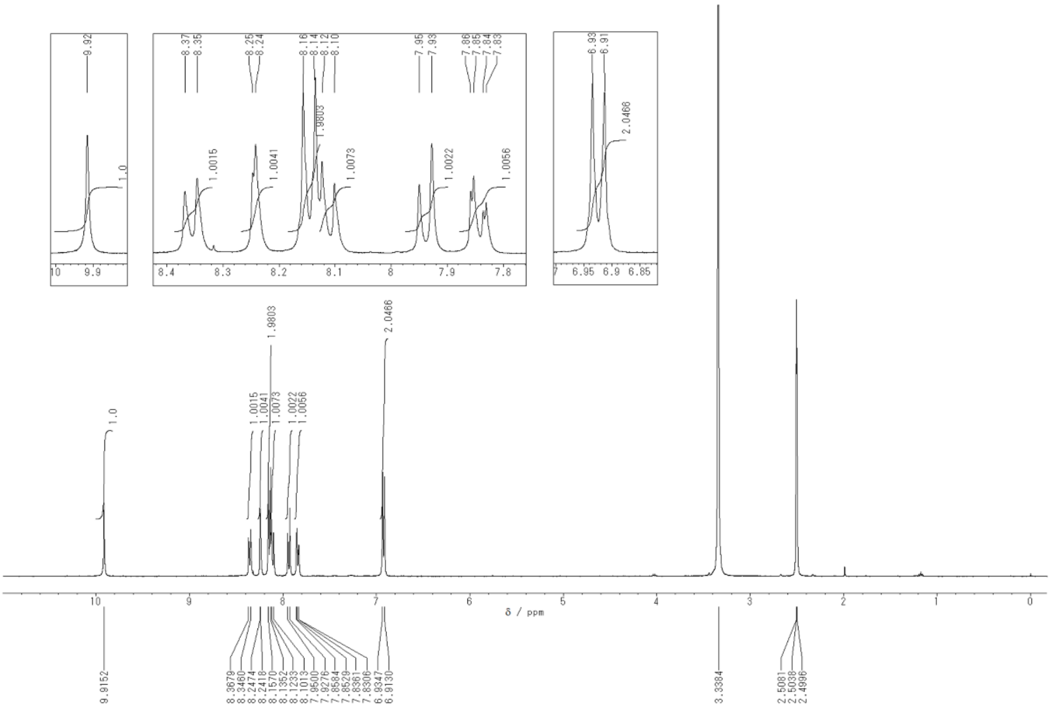

Chart S1 ^{1}H NMR spectrum of compound **4** in DMSO-d_6 at 293 K.

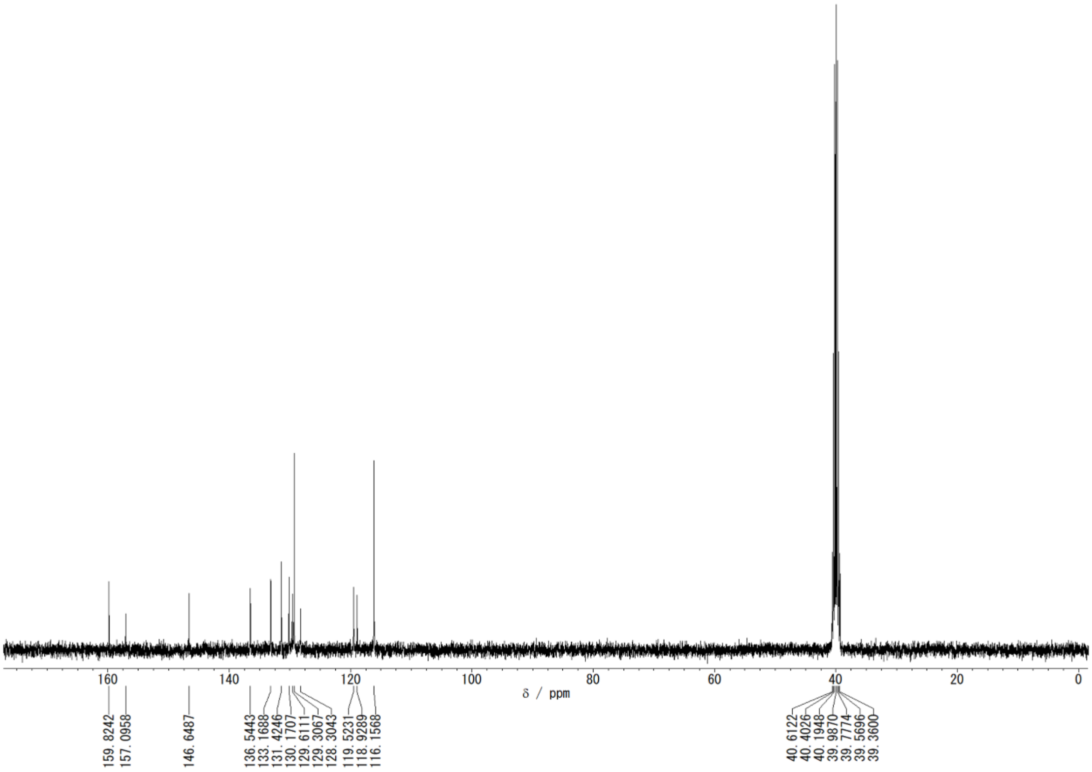

Chart S2 ^{13}C NMR spectrum of compound **4** in DMSO-d_6 at 293 K.

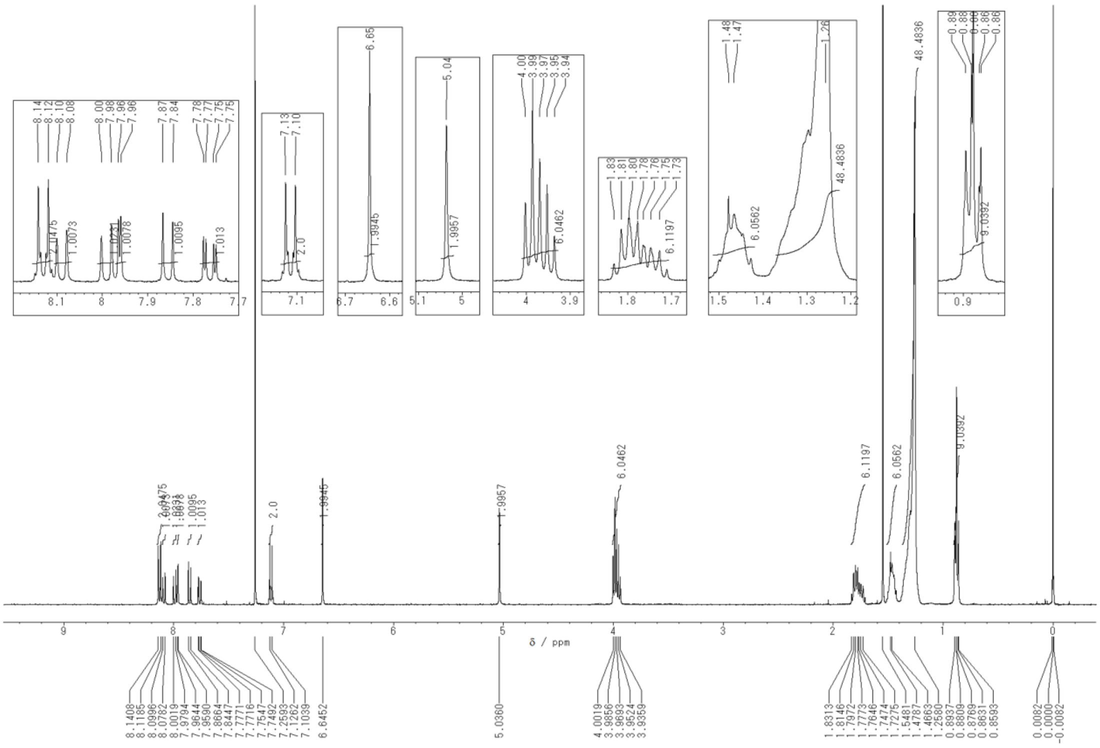

Chart S3 ^{1}H NMR spectrum of compound **5** in $CDCl_3$ at 293 K.

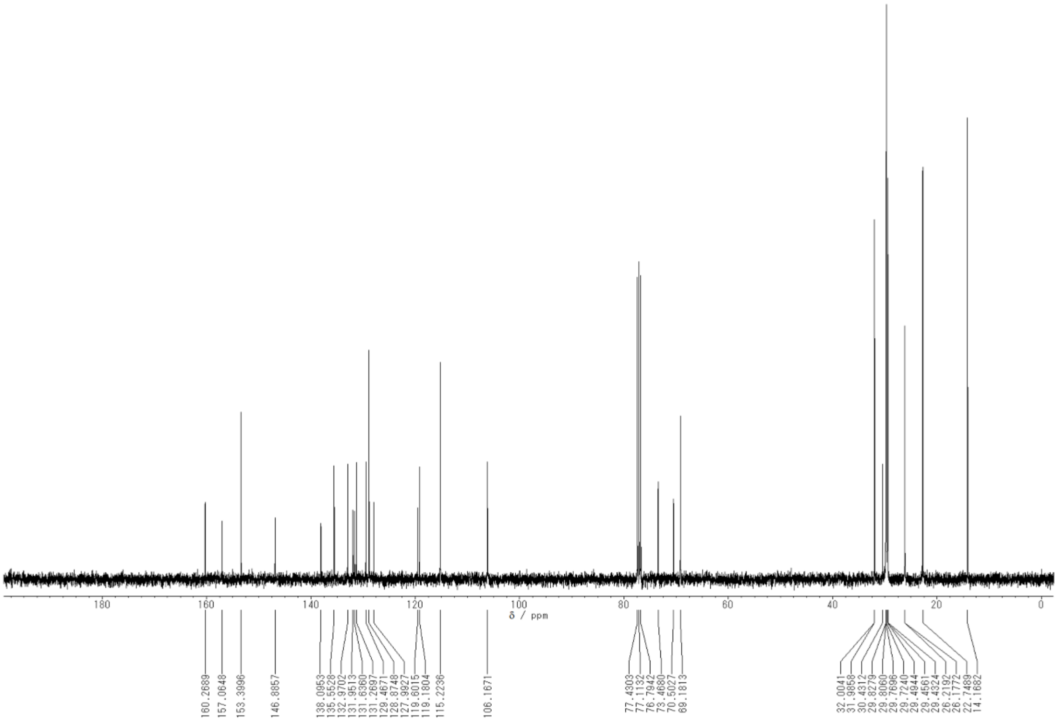

Chart S4 ^{13}C NMR spectrum of compound **5** in $CDCl_3$ at 293 K.

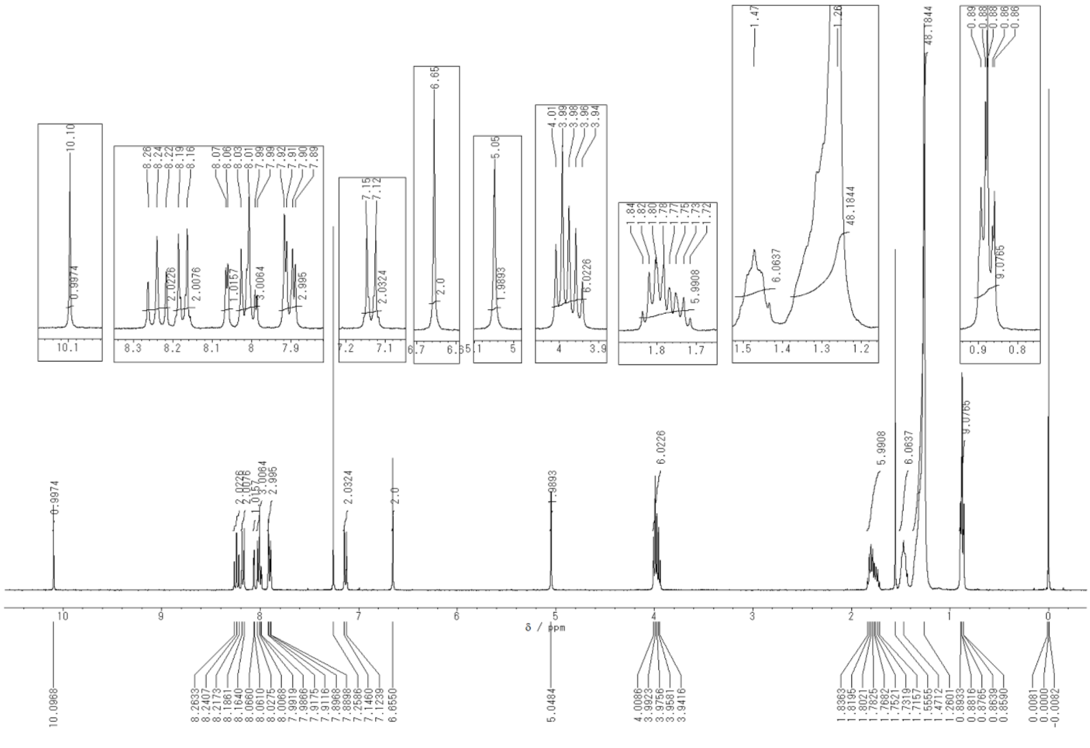

Chart S5 ^{1}H NMR spectrum of compound **6** in $CDCl_3$ at 293 K.

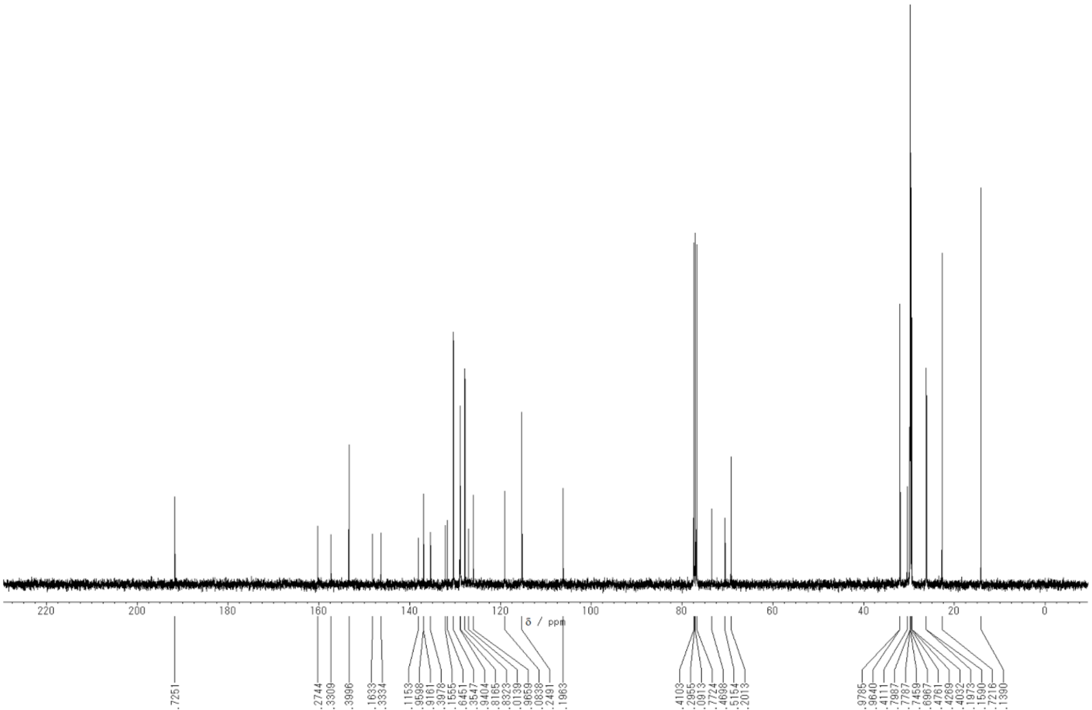

Chart S6 ^{13}C NMR spectrum of compound **6** in $CDCl_3$ at 293 K.

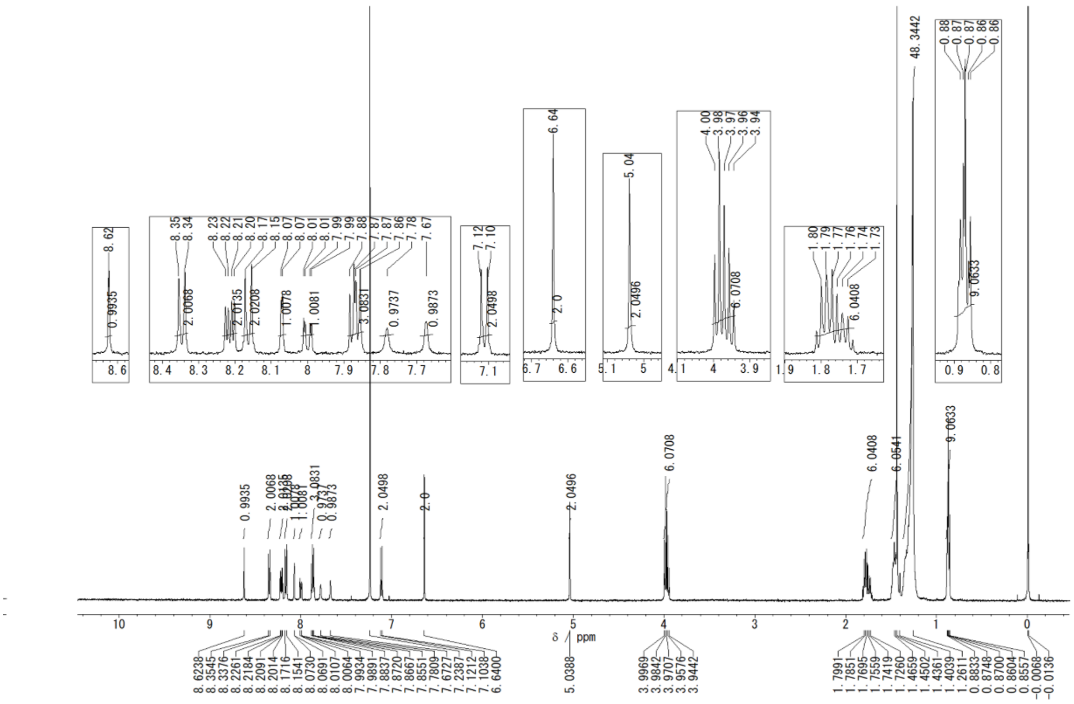

Chart S7 ^{1}H NMR spectrum of compound **2** in $CDCl_3$ at 333 K.

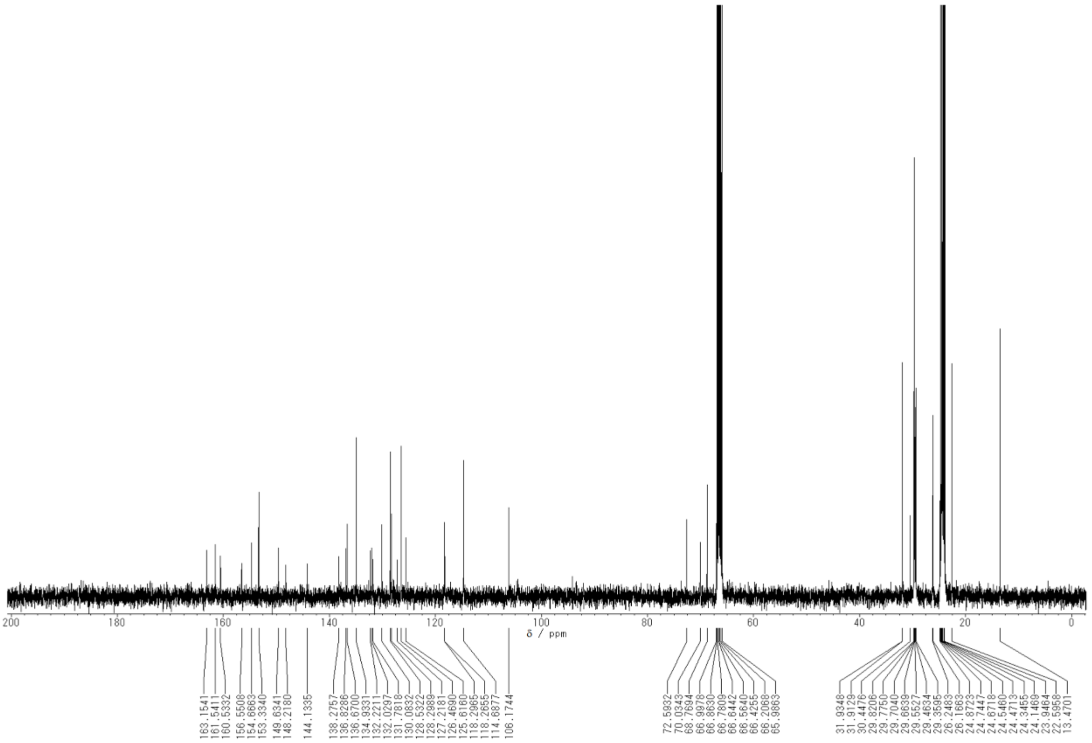

Chart S8 ^{13}C NMR spectrum of compound **2** in THF-d_8 at 293 K.

Supplementary Figures

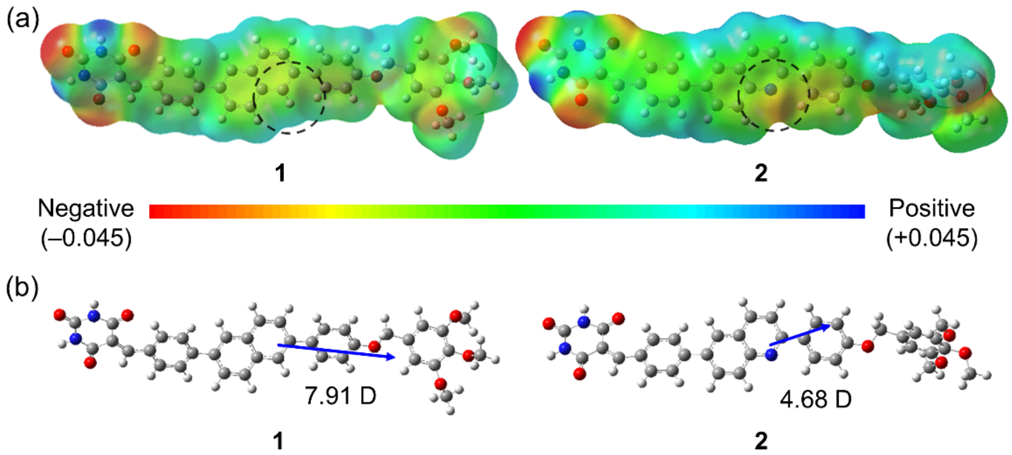

Fig. S1. (a) Molecular electrostatic potentials of molecules **1** and **2** in MCH. The surface color implies charge density. (b) Optimized structures of **1** and **2** in MCH. The blue arrows in the optimized structures represent directions and magnitudes of permanent dipole moments. All DFT calculations were carried out with the B3LYP/6-31G(d) basis set with IEF-PCM model.

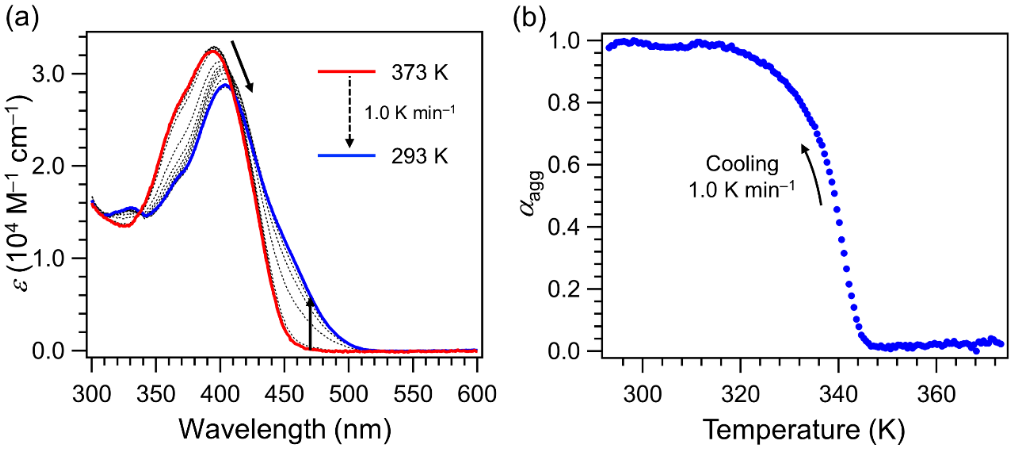

Fig. S2 (a) Temperature-dependent absorption spectra of **2** ($c = 5.0 \times 10^{-6}$ M) in MCH upon cooling from 373 to 293 K at a rate of 1.0 K min^{-1}. (b) Cooling curve of **2** ($c = 5.0 \times 10^{-6}$ M) obtained by plotting the mole fraction of the aggregated molecules (α_{agg}, calculated from the absorption change at 470 nm) as a function of temperature in MCH.

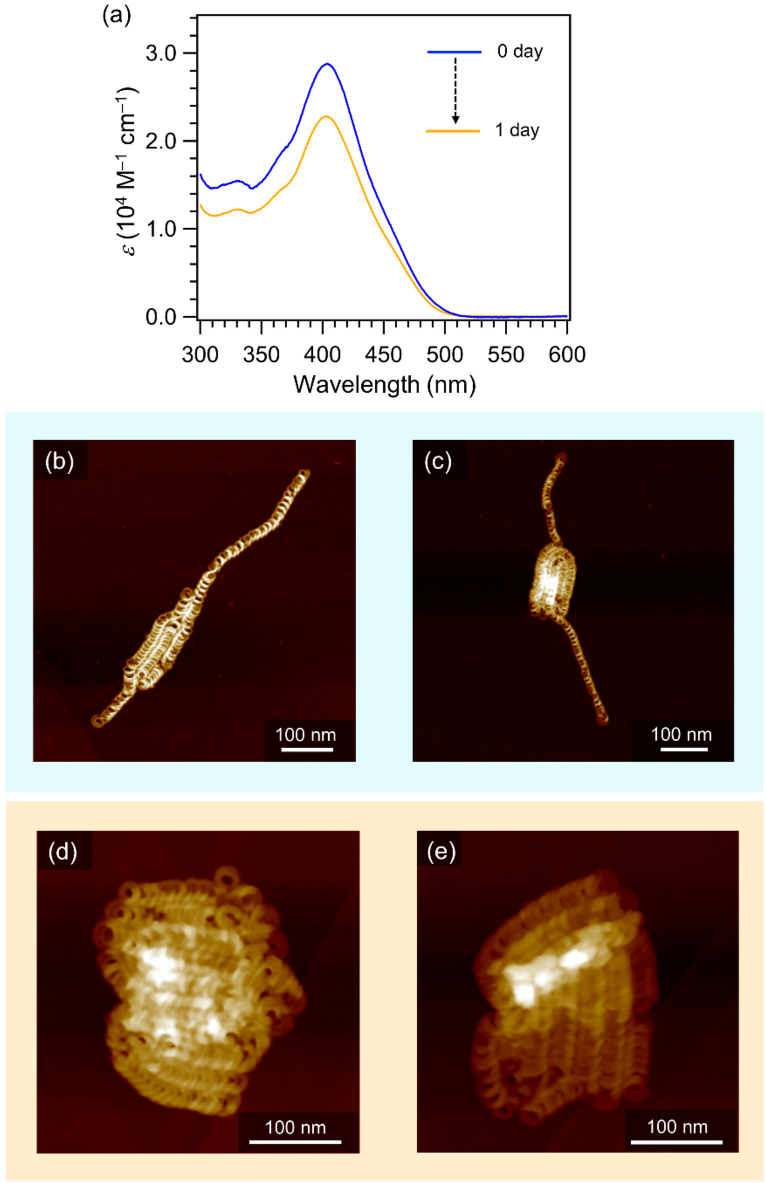

Fig. S3 (a) UV/vis absorption spectra of a MCH solution of **2** ($c = 5.0 \times 10^{-6}$ M) just after cooling from 293 K at a cooling rate of 1.0 K min^{-1} and after aging for 1 day. (b–e) AFM images of $\mathbf{SP}_{\text{helicoid}}$ of **2** (b,c) just after cooling and (d,e) after aging for 1 day.

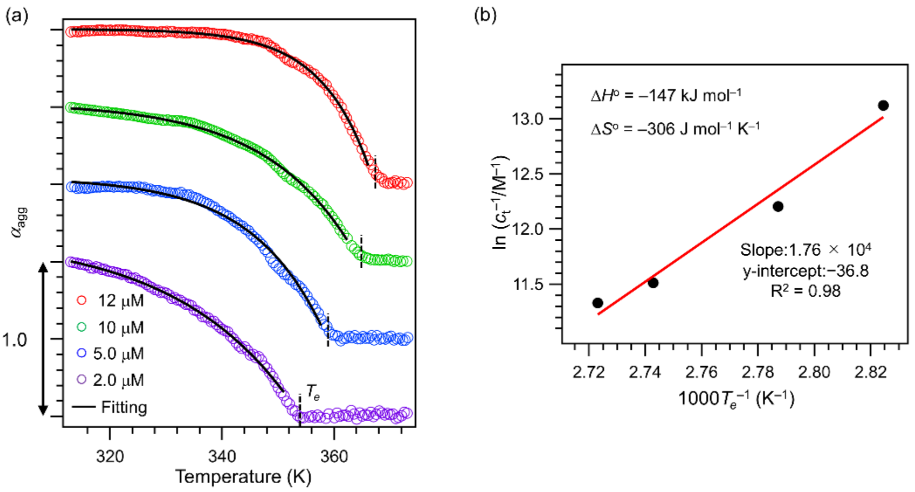

Fig. S4 (a) Heating curves of 1-day aged **SP**helicoid of **2** (c = 2.0, 5.0, 10, and 12 × 10^{-6} M) obtained by plotting the α_{agg} (estimated from the absorption changes at 470 nm) as a function of temperature in MCH. The black curves show the cooperative elongation model fit.[S2] (b) van't Hoff analysis of **SP**helicoid of **2** by plotting natural logarithm of the monomer concentrations as a function of T_e^{-1}. The T_e values were determined by the cooperative elongation model fit. The red line shows the corresponding linear fit. The analysis provided thermodynamic parameters including standard enthalpy ($\Delta H°$ = −147 kJ mol^{-1}), entropy ($\Delta S°$ = −306 J K^{-1} mol^{-1}), and Gibbs free energy ($\Delta G°$ = −56 kJ mol^{-1}) at 298 K.

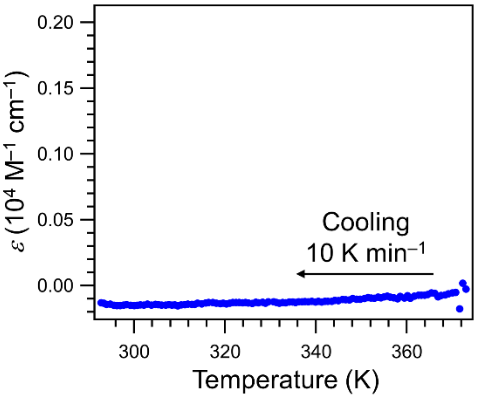

Fig. S5 Temperature-dependent change of molar extinction coefficient (ε) of **2** (c = 1.0 × 10^{-5} M) at λ = 470 nm in 40% toluene/MCH (v/v) upon cooling from 373 K to 293 K at a rate of 10 K min^{-1}.

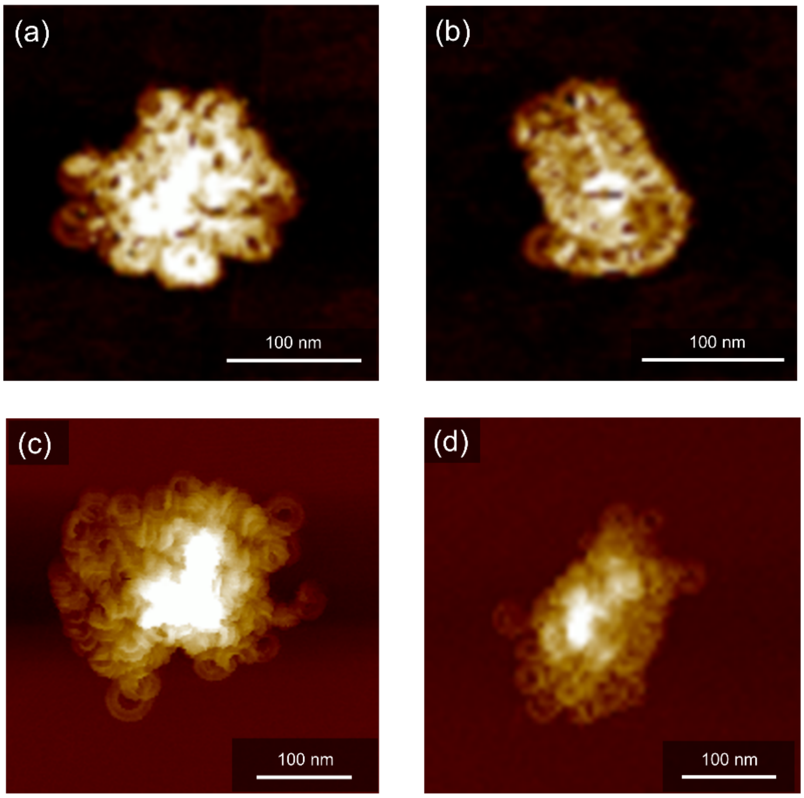

Fig. S6 (a–d) AFM images of $\textbf{SP}_{\text{helicoid}}$ obtained by cooling a hot 40% toluene/MCH (v/v) solution of **2** ($c = 1.0 \times 10^{-5}$ M) from 373 to 293 K at a cooling rate of 10 K min^{-1}. The solutions were aged at 293 K for 2000 s after cooling.

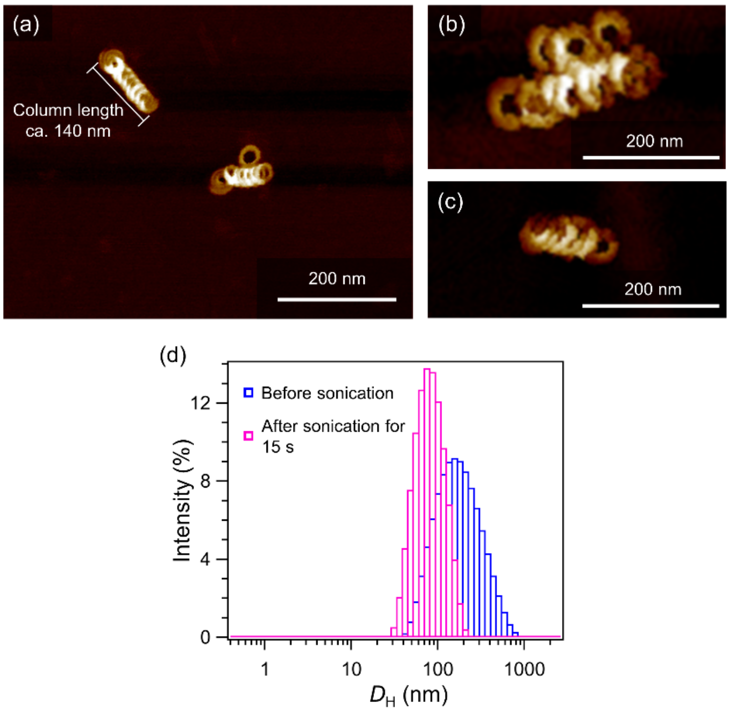

Fig. S7 (a–c) AFM images of $\mathbf{SP}_{\text{helicoid}}$ seeds of **2** prepared by sonicating $\mathbf{SP}_{\text{helicoid}}$ in MCH. (d) DLS size distribution of the original $\mathbf{SP}_{\text{helicoid}}$ solution (blue) and the $\mathbf{SP}_{\text{helicoid}}$ seed solution obtained by sonication (pink).

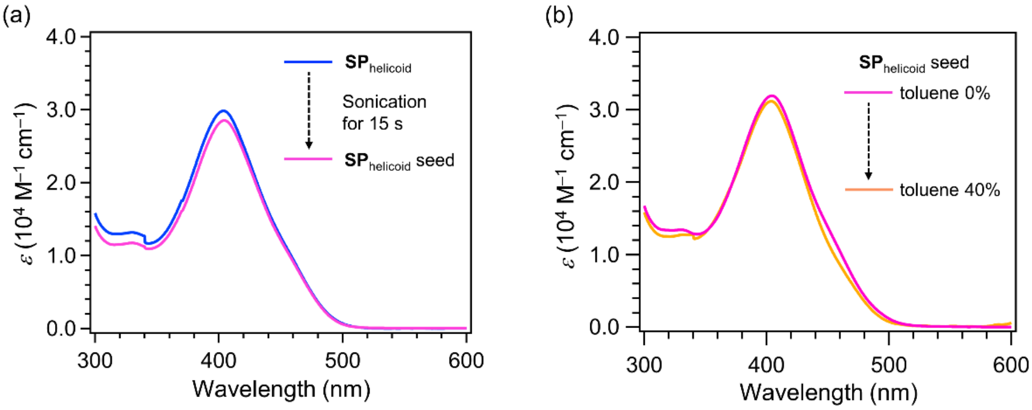

Fig. S8 (a) UV/vis absorption spectra of $\mathbf{SP}_{\text{helicoid}}$ solution of **2** in MCH before (blue) and after sonication (pink). (b) UV/vis absorption spectra of $\mathbf{SP}_{\text{helicoid}}$-seeds in MCH (pink) and in 40% toluene/MCH (v/v) (orange).

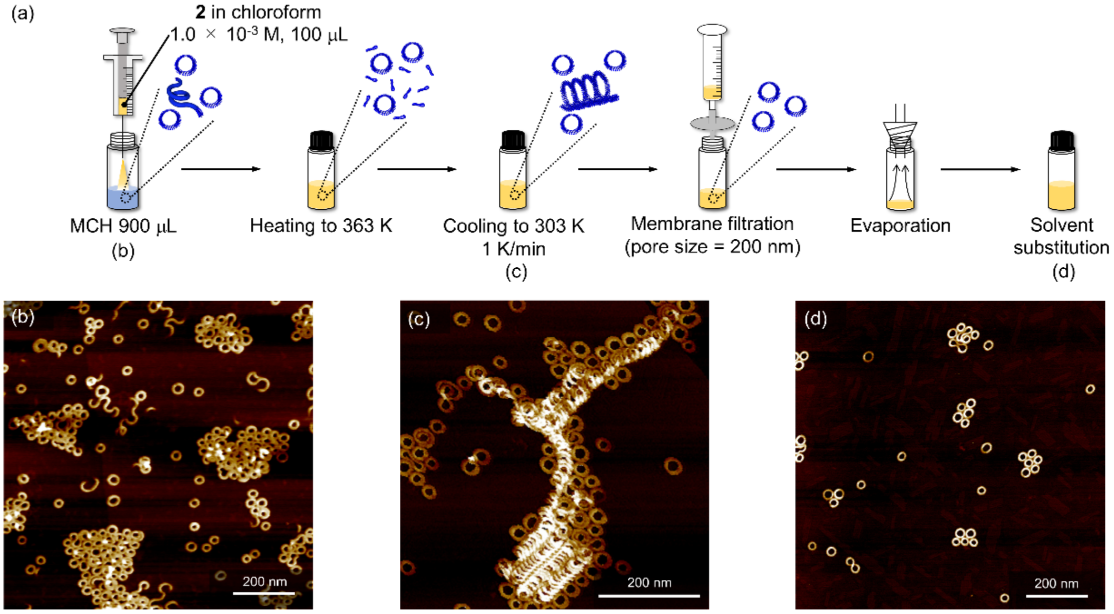

Fig. S9 (a) Schematic representation of the protocol to purify $\mathbf{SP}_{\text{ring}}$ from a mixture with open-ended fibers. (b–d) AFM images of the samples at different steps shown in (a).

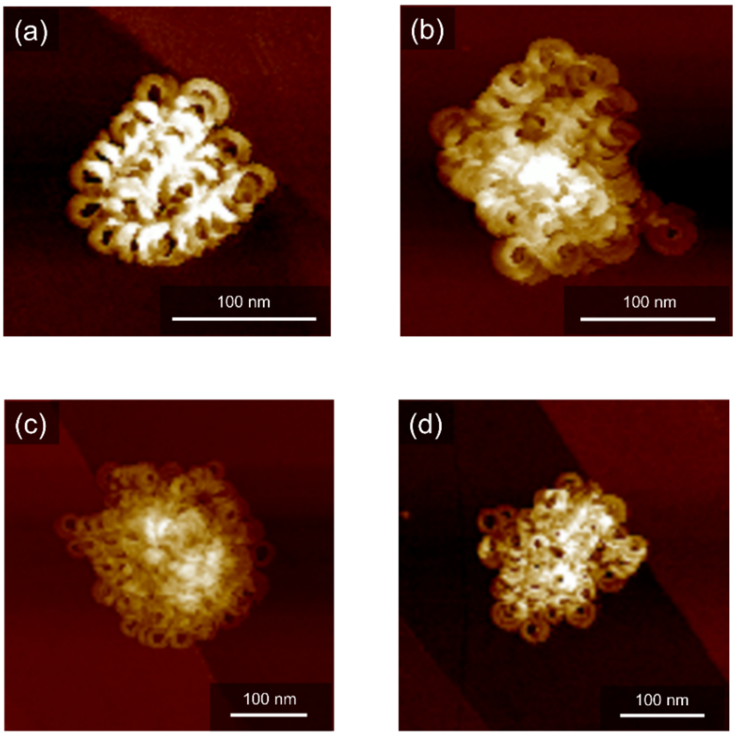

Fig. S10 (a–d) AFM images of **SP**$_{\text{helicoid}}$ of **2** obtained by adding **SP**$_{\text{helicoid}}$ seeds (c = 1.0 × 10^{-5} M) to the as-cooled supersaturated solution of **2** (c = 1.0 × 10^{-5} M) in 40% toluene/MCH (v/v) at 297 K.

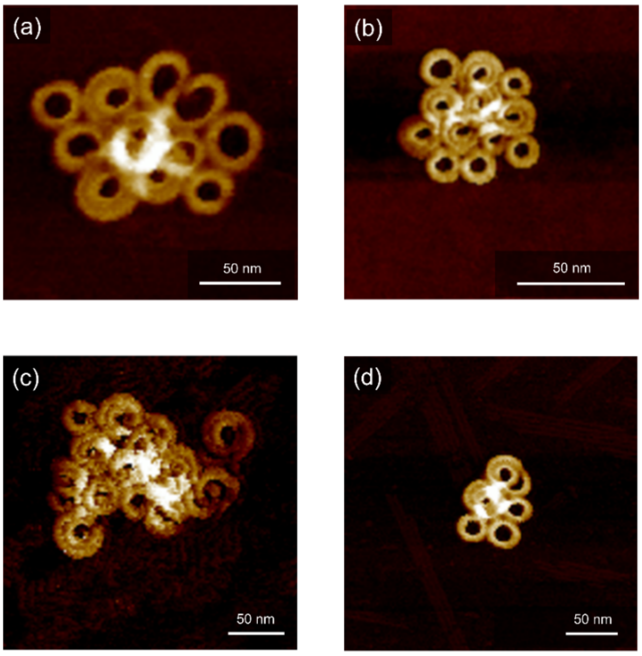

Fig. S11 (a–d) AFM images of **SP**$_{\text{random}}$ of **2** obtained by adding **SP**$_{\text{ring}}$ seeds ($c = 1.0 \times 10^{-5}$ M) to the as-cooled supersaturated solution of **2** ($c = 1.0 \times 10^{-5}$ M) in 40% toluene/MCH (v/v) at 297 K.

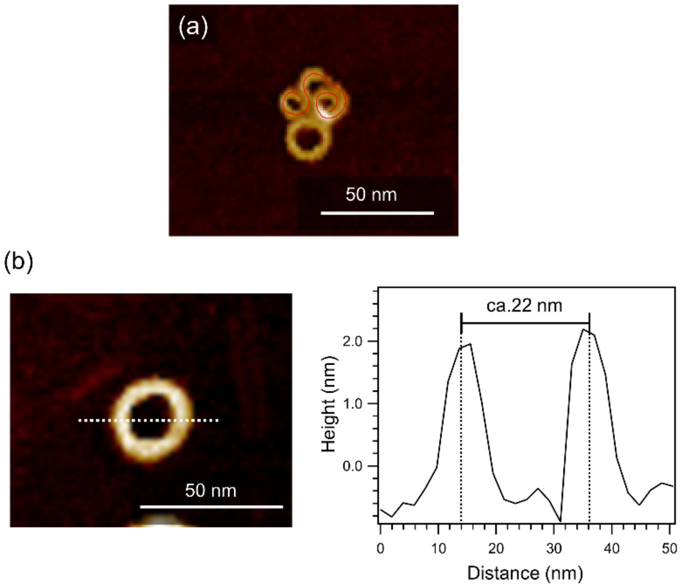

Fig. S12 (a) Tracing red lines measure the length of fibers in the AFM image of **SP**$_{\text{ring}}$-seeded solution after equilibration. (b) AFM image and AFM cross-sectional analysis of **SP**$_{\text{ring}}$ seed in 40% toluene/MCH (v/v).

Supplementary Table

Table S1 Kinetic parameters and mean squared error (MSE) of the seeded experiments obtained by growth curve fitting using AmyloFit software (http://www.amylofit.ch.cam.ac.uk).[S3]

Seed	k_+k_n ($M^{-1.3}s^{-2}$)	k_+k_2	n_c	n_2	MSE
Unseeded	0.68	8.4×10^3 ($M^{-1.9}s^{-2}$)	1.3	0.9	0.0008
SP$_{\text{ring}}$-seeded	6.5	2.2×10^7($M^{-2.4}s^{-2}$)	1.3	1.4	0.0003
SP$_{\text{helicoid}}$-seeded	73		1.3		0.0001

Supporting reference

[S1] M. J. Frisch, G. W. Trucks, H. B. Schlegel, G. E. Scuseria, M. A. Robb, J. R. Cheeseman, G. Scalmani, V. Barone, G. A. Petersson, H. Nakatsuji, X. Li, M. Caricato, A. V. Marenich, J. Bloino, B. G. Janesko, R. Gomperts, B. Mennucci, H. P. Hratchian, J. V. Ortiz, A. F. Izmaylov, J. L. Sonnenberg, D. Williams-Young, F. Ding, F. Lipparini, F. Egidi, J. Goings, B. Peng, A. Petrone, T. Henderson, D. Ranasinghe, V. G. Zakrzewski, J. Gao, N. Rega, G. Zheng, W. Liang, M. Hada, M. Ehara, K. Toyota, R. Fukuda, J. Hasegawa, M. Ishida, T. Nakajima, Y. Honda, O. Kitao, H. Nakai, T. Vreven, K. Throssell, J. A. Montgomery, Jr., J. E. Peralta, F. Ogliaro, M. J. Bearpark, J. J. Heyd, E. N. Brothers, K. N. Kudin, V. N. Staroverov, T. A. Keith, R. Kobayashi, J. Normand, K. Raghavachari, A. P. Rendell, J. C. Burant, S. S. Iyengar, J. Tomasi, M. Cossi, J. M. Millam, M. Klene, C. Adamo, R. Cammi, J. W. Ochterski, R. L. Martin, K. Morokuma, O. Farkas, J. B. Foresman, and D. J. Fox, *Gaussian 16* (*Revision B.01*), Wallingford CT, 2016.

[S2] P. Jonkheijm, P. van der Schoot, A. P. H. J. Schenning, and E. W. Meijer, *Science*, 2006, **313**, 80-83.

[S3] G. Meisl, J. B. Kirkegaard, P. Arosio, T. C. T. Michaels, M. Vendruscolo, C. M. Dobson, S. Linse and T. P. J. Knowles, *Nat. Protoc.*, 2016, **11**, 252–272.

[S4] V. Percec, M. Peterca, Y. Tsuda, B. M. Rosen, S. Uchida, M. R. Imam, G. Unger and P. A. Heiney, *Chem. Eur. J.*, 2009, **15**, 8994–9004.